

NANO-WEAR AND NANO-FATIGUE WEAR TESTS

Raymond Hsiao and D. B. Bogy
Computer Mechanics Laboratory
Department of Mechanical Engineering
University of California at Berkeley
Berkeley, CA 94720

C. Singh Bhatia
Storage Systems Division
IBM, 5600 Cottle Road
San Jose, CA 95193

ABSTRACT

The nano-wear behaviors of carbon and silver coatings on air-bearing slider rails and nitrogenated carbon films with different deposition bias on disks were studied. Nano-wear tests were also performed on a diamond-like carbon (DLC) film for which the mechanical properties vary along the thickness direction. We also continue a previous investigation of frictional material build-up on Si samples with different orientations in a controlled environment. Frictional material build-up was found on Si<100> and Si<111> but not on Si<110>. Nano-fatigue wear tests using the Point Contact Microscope(PCM) in the environmental chamber showed that the amount of frictional build-up increased significantly in the presence of oxygen, implying that this frictional build-up formation is an oxidization process.

1 Introduction

Nano-wear tests with the PCM were first proposed by Miyamoto et al. (1992) and Miyake et al. (1992)¹ to investigate the wear resistance of C⁺-implanted silicon and carbon films with silicon inclusion and fluorination. Many investigations have shown that this technique is effective for evaluating microscale tribological properties, especially wear durability of ultra-thin films for magnetic recording applications (Jiang et al., 1995; Miyamoto et al., 1995)^{2, 6}. The generic term of protective coatings on magnetic disks refers to a variety of materials, structures and performance characteristics which result from different processes and compositions used in the fabrication of the films. As is the case for the technical properties, the wear performance of these protective coatings depends on the structure of the films, as well as the materials and lubricants of the HDI. Previous research²⁻⁵ on nano-wear tests has yielded some valuable information about microscale surface features and properties. Nevertheless, further fundamental understanding of nano-wear on different materials is needed, since selecting proper and efficient characterization parameters for nano-wear tests requires a clear identification of the dominant wear patterns. In this report, nano-wear tests were conducted on carbon and silver coatings on air-bearing slider rails, and nitrogenated carbon films deposited with different bias on disks were also studied. It was found that the deposition density and bias are important for determining the wear resistance performance in the nano-wear tests.

Although Scanning Probe Microscopes (SPM) have been widely used to evaluate a variety of materials, there remain several unexplained observations. Furthermore, most solid surfaces in air adsorb water, are contaminated by organic materials or react with the

gaseous environment under certain circumstances. Surface finishings, such as polishing, grinding, cutting, and etching, produce surface layers whose properties differ from those of the bulk material. These complicated surfaces are the “real” sliding surfaces. From a previous study of nano-fatigue wear tests, an unexpected material build-up was found on a silicon<100> sample under raster scanning or single-line scanning repeatedly with a diamond tip when the normal load is less than the critical load for wear initiation (Jiang, Hsiao and Bogy, 1995)^{3, 4}. Further investigations of nano-fatigue wear on Si with different orientations and under various environmental conditions are included here. The study of nano-fatigue wear in the environmental chamber attributed this frictional layer build-up on Si to an oxidization process during the repeated scanning with the appropriate load.

2 Experiments and Results

A. Nano-Wear Tests on Carbon and Silver coated Al₂O₃-TiC Air-Bearing Sliders

Two different coatings, silver and carbon, were deposited on the rails of Al₂O₃-TiC sliders at two deposition densities, 5×10^{16} atom / cm² and 3×10^{16} atom / cm². For convenience, the silver coated sliders with deposition densities of 5×10^{16} atom / cm² and 3×10^{16} atom / cm² are referred to hereafter as slider #1 and #2, respectively, and the carbon coated sliders with deposition densities of 5×10^{16} atom / cm² and 3×10^{16} atom / cm² are referred to as slider #3 and #4, respectively. The slider material is Al₂O₃-TiC, which contains Al₂O₃ as a matrix material embedded with TiC grains with a range of diameters of about 0.1 ~ 2 μm. The TiC grains are usually 0.3 ~ 1.0 nm higher than the

Al₂O₃ matrix because of the difference in wear rates during polishing. Nano-wear tests on such a material show diverse behavior under different normal loads, due to the grain structure, heterogeneous phase properties, film strength and film adhesion. In performing a nano-wear test on these Al₂O₃-TiC sliders using the PCM, we first scan the surface of an area of 5 μm × 5 μm with a light load, in order to obtain the surface topography image. Then the scan size is reduced to 2 μm × 2 μm, centered at the same location, and the loading force is increased to a pre-determined value. After a wear cycle, the loading force and scan size are reset to their original values and the surface topography is again obtained. The wear depth can be acquired from the cross section of the wear mark. The wear depth versus loading force is plotted in Fig. 1 for all four sliders to compare the wear resistance of the different films. All tests were performed in ambient environment, with temperature between 22° C and 26° C, and humidity between 34% and 41%. The radius of the diamond tip was around 100 nm, and the cantilever spring constant was about 36.1 N/m. During the scratching process, the tip scanning frequency was 1 Hz. Therefore, the average sliding speed in the lateral direction was 4 μm/sec., while the scan pitch in the longitudinal direction was 7.8 nm. It is shown in Fig. 1 that the role of the loading force on determining the wear resistance in the nano-wear tests is important. For a light load (less than 38 μN), both the carbon and silver coatings were removed uniformly and gradually. For a higher load, however, these films behaved quite differently. The wear depth for slider #3 rapidly increased after 38 μN indicating that this film completely loses its protective capacity, which leads to a sudden collapse inside the wear mark under these loads. On the other hand, the coatings on the other three sliders became progressively thinner, as the load increased, with the wear depth of slider #4

remaining less than that of sliders #1 and 2, which are the silver coated sliders, until the loading force reached 110 μN . Above that load the wear depth of slider #4 went up rapidly with load, in a fashion similar to that of slider #3 above 38 μN . There is no significant difference in the nano-wear test results between the two silver coated sliders. The results imply that for the loading force less than 110 μN , the carbon coated slider with density of 3×10^{16} atom / cm^2 tends to provide better protection from damage during sliding contact. For higher contact loads, the results suggest that silver coatings are more resistant to wear than the carbon coatings and therefore may be better choices as wear protective overcoats than carbon.

B. Nano-Wear Tests on CN_x coated disks

CN_x overcoats fabricated with 0, -50, -100 and -150V substrate bias during film growth were tested. These were supersmooth disks with film thickness of 7.5 nm. All tests were performed in ambient environment. The radii of the diamond tips were around 100 nm, with spring constants of about 90.8 N/m and 48.3 N/m. During the scratching process, the tip scanning frequency was 1 Hz. The average sliding speed in the lateral direction was 2 $\mu\text{m}/\text{sec}$., while the scan pitch in the longitudinal direction was 3.9 nm. The hardness values and surface images of these films were measured by a different SPM (not the PCM), the Hysitron tester. The hardness were determined by the residual depths, which were in the range from 1.5 nm to 4.5 nm. The indentation force was 15 μN with a triangle loading profile and a diamond tip of 50 nm tip radius. As shown in Fig. 2, the indentation residual depths of the CN_x overcoats with 0, -50, -100 and -150V substrate bias were 4.5 nm, 1.5 nm, 2 nm and 2.6 nm, respectively. The differences in the

hardnesses of the films are apparent from the differences in the residual depths, which indicates that the CN_x overcoat with -50 V substrate bias has the highest value of relatively hardness, with a residual depth as small as 1.5 nm, while the softest overcoat resulted from 0 V bias. The surface roughness of these films was also measured, and they are plotted in Fig. 3, which depicts the RMS roughness for a $2\ \mu\text{m} \times 2\ \mu\text{m}$ scan size for each deposition substrate bias. It is observed that the surface roughness of these CN_x coated disks is significantly influenced by the substrate bias during the stages of film growth, with rougher surfaces for higher substrate bias. Since the disk substrates roughnesses are assumed to be about the same, the film roughness difference can be attributed to the bias differences, with rougher films resulting for lower deposition energy. As mentioned in the previous section, it is well established that the loading force plays a very important role in the nano-wear tests. In the nano-wear test on these CN_x coated disks, two different loads were used to investigate the wear mechanisms. With 23 μN applied to a diamond tip, using the PCM with a nominal radius of 100 nm, we compared the wear resistance of these films. The wear depths after one wear cycle are plotted in Fig. 4. Each value in Fig. 4 represents the average of two independent tests. These results are consistent with the previous nano-indentation hardness measurements, which showed that the 0 V bias film is the softest one, the -50 V film is the hardest one and hardness decreases with the substrate bias thereafter. A comparison of wear depths after one wear cycle on these films at 63 μN load is illustrated in Fig. 5, where it is seen that the wear depth decreases with deposition bias monotonically, the most wear resistant one being that for -150 V bias. It is believed that the mode of failure due to film adhesion is largely neglected in the nano-wear test with relatively lighter loads. For lighter loads

presumably below the threshold of cracking, the diamond tip is essentially scratching on the very top surface of the film without any effect of the substrate, and the nano-wear tests are in agreement with the nano-indentation hardness results. As the loading force goes up, micro crackings occur by film bending as the diamond tip passes by and forms chips that drop out, causing sever damage to the relatively softer substrate, especially for the case of weak film adhesion.

C. Nano-Wear Tests on Diamond-like Carbon Films

Diamond-like Carbon(DLC) was deposited on a Si<100> substrate using vacuum arc discharge of a graphite cathode with an arc current of 300 A, pulse duration of 5 ms and pulse repetition rate of 1 Hz. The Si sample was attached to a water-cooled steel sample holder. A 90 degree bent macroparticle filter was used to filter out the macro-size particles during the plasma deposition. The substrate was repetitively biased to a voltage of -100 volts, pulse duration of 2 μ s, repetition rate of 2 Hz and pulse duty cycle of 33%. The base pressure was 8×10^{-6} Torr. The final thickness of the DLC coating was about 10 nm. Nano-indentations using the PCM were performed on the DLC film and Si<100>. The DLC film, with a hardness of about 47 Gpa, is considerably harder than most of the other carbon films. In performing a nano-wear test on the DLC film using the PCM, the surface of an area of $2 \mu\text{m} \times 2 \mu\text{m}$ was scanned with a light load, in order to obtain the surface topography image. Then the scan size was reduced to $1 \mu\text{m} \times 1 \mu\text{m}$ at the same location, and the loading force was increased to a pre-determined value. After two wear cycles, the loading force and scan size were reset to their original values and the surface

topography was obtained. The wear depth can be acquired from the cross section of the wear mark. The wear depths versus wear cycles with two different loads are plotted in Fig. 6 to compare the wear resistance of this film. All tests were performed in ambient environment. The radius of the diamond tip was around 100 nm, with a spring constant of about 61.9 N/m. During the scratching process, the tip scanning frequency was 1 Hz. Therefore, the average sliding speed in the lateral direction was 2 $\mu\text{m}/\text{sec.}$, while the scan pitch in the longitudinal direction was 7.8 nm. From Fig. 6, nano-wear scratching with a load of 100 μN was hardly enough to modify the film surface, with wear depths around 1 nm for up to 30 cycles, strongly indicating the property of superior scratch resistance on this film. The scratched area with this load formed bump-type nano-irregularities as shown in Fig. 7. A somewhat similar wear surface has been reported by Khurshudov and Kato for polycarbonate material using the AFM⁷. A model, based on crack formation and growth was suggested to explain these phenomena by the authors. The rate of nano-wear with a load of 200 μN , however, is entirely different and can be divided into three distinct zones. With the 200 μN load, the diamond tip uniformly and slowly abraded material from the surface until about 20 cycles. After 20 cycles the diamond tip started to chip off the surface, as shown in Fig. 8, and went deeper at a faster rate. Nano-wear tests were also performed on bare Si with a load of 200 μN applied to the same tip using the PCM. It is noted that the wear rate on the DLC film after 26 cycles was about the same as that of on bare Si. This is seen by carefully computing the slope from the wear verse cycle plot, indicating that the diamond tip was scratching on the Si substrate after the 26th cycle. The curve with three different slopes showed that there are multiple layers on the DLC sample. In the thickness direction, they are from the top to 6 nm deep, representing a

toughest carbon-carbon bonding structure, and from 6 nm to about 18 nm representing a relatively softer silicon-carbide bonding structure. Since the film thickness is only 10 nm, it is implied that carbon atoms were deposited as deep as 8 nm underneath the Si substrate during the plasma deposition process.

D. Nano-Fatigue Wear Tests in Ambient Environment

D.1 “Frictional Build-up” on Si

Two nano-fatigue wear methods were adopted: raster scanning nano-fatigue wear tests and single-line scanning nano-fatigue wear tests. In these tests, a diamond tip is controlled to scan over a few micrometers square area with a normal load smaller than the critical load for wear initiation. Then the surface topography of a larger area is measured with the same tip. The wear information can be obtained from the measured image. For single-line fatigue wear tests, the tip sliding is repeated in the same track on the surface with a normal load smaller than the critical load for wear initiation. Similarly, after these wear tests, the surface is measured and analyzed. Single-line fatigue wear tests with 15 μN and 2000 wear cycles were performed on Au , SiO_2 , C, and Si<100> in an ambient laboratory environment, where the temperature was between 26 ~ 30 °C, and the humidity was about 40 ~ 45%. The results are plotted in Fig. 9. On the silicon sample, with the orientation of <100>, the interaction contact area on the surface was raised rather than depressed after the tests, or frictional build-up occurred since the depth is “negative” as illustrated in Fig. 9. Frictional build-up was also found on Si with a <111> orientation in more recent nano-fatigue wear tests. Fig. 10 shows that the whole scratched area, 2 μm

$\times 2 \mu\text{m}$, was raised by 1.9 nm on p-type Si<111> after 200 wear cycles with 30 μN load applied to a diamond tip. It should be noted that the frictional layer build-up behavior is not observed when nano-fatigue wear tests are performed on silicon with a <110> orientation. The behaviors of frictional build-up were well established recently by Jiang et al.^{4,5} in which it was revealed that the frictional layer build-up was noticeable harder than silicon, and its amount was proportional to wear cycles and loading force in certain ranges. However, the origin of the frictional build-up on Si <100> and Si <111>, but not on Si <110>, has remained an open question.

D.2 Observation of “Frictional Build-up using an AFM

In order to precisely locate the AFM tip to the region of frictional build-up produced by the PCM, we used an etching process to form a 20 μm wide, 2 cm long and 100 nm high “cross” on Si for a reference coordinate, as shown in Fig. 11. Single-line nano-fatigue wear tests were performed and observed using the PCM near the corners of the “cross” as shown in Fig. 12. Then the sample was moved to the DI Nanoscope II AFM. Since the “cross” is a 100 nm high platform, it can be easily located with a 300 magnification microscope under this system. In this way, we successfully observed the frictional build-up that is shown in Fig. 13 and measured its height to be about the same height as that measured by the PCM. As shown in Figs.12 and 13, a particle located at the left center and a deep longitudinal scratch located in the upper right provide verification that we were observing the same frictional build-up.

E. Nano-Fatigue Wear Tests on Si <100> in an Environmental Chamber

Motivated by the possible environmental effects on the frictional build-up formation during the nano-fatigue wear tests on Si, we placed the PCM in a chamber, which is a Plexiglas box with several ports for passing gases and electrical signals through the chamber wall. High purity gases (< 100 PPM) were available in compressed cylinders for filling the chamber. Humidity and temperature were measured by a sensor, placed inside the chamber. Nano-fatigue wear tests were then performed in the environmental chamber filled with oxygen, nitrogen or argon. Due to the high purity of the gas, the humidity inside the chamber dropped to 4% from 42% after slowly passing the gas for 10 hours, while the temperature remained about the same at the range of 26 - 28° C. Single-line nano-fatigue wear tests, 1 μm long repeated sliding, using a 30 μN load for 5000 wear cycles were performed on Si $\langle 100 \rangle$ under these single gas environments. Frictional build-up “depths“ were measured and plotted in Fig.14. Nano-fatigue wear test results on Si $\langle 100 \rangle$ in the laboratory environment with the same testing conditions were also included for comparison. As shown in Fig.14, the amount of frictional build-up is increased by about 60%, in terms of build-up height, in an O_2 environment. Although friction build-up was still produced in a N_2 or Ar environment, the amount is noticeably less than the case under the laboratory environment. These results suggest that the frictional layer build-up formation is related to oxidization. It is believed that the observation of the frictional build-up produced under the N_2 or Ar environments is mainly due to the unavoidable O_2 exposure and absorption prior to the tests.

3 Conclusions

1. Comparing carbon and silver coated slider from the nano-wear test results, that a carbon coated slider with 3×10^{16} atom / cm² deposition density has a better wear resistance when the load is less than 110 μ N. In the case of nano-wear test with load greater than 110 μ N, silver coated sliders were more wear resistant. There is no significant difference in the nano-wear test performance between the silver coated sliders with deposition densities of 3×10^{16} atom / cm² and 5×10^{16} atom / cm².
2. Similar to the slider overcoats, the CN_x coatings on disks behave differently in the nano-wear tests with different loads. For a light load, the nano-wear test results are consistent with the nano-indentation test results with the -50 V bias overcoat being the hardest and 0V being the softest one. In the high loading case, -150 V film is the most wear resistant one and the film strength decreases with the bias.
3. There are multiple layers with distinct mechanical properties on the DLC film on Si along its thickness direction.
4. Frictional build-up was found on Si <100> and Si <111> but not on Si <110> using the PCM. Frictional build-up was also observed under the commercial AFM and it was found to agree with the observed results using the PCM.
5. The amount of frictional build-up increased significantly in an O₂ environment, which suggests that oxidization processes have taken place during the nano-fatigue wear tests on Si.

4 List of Figures

Fig. 1 Wear depth versus loading force on carbon and silver coated sliders.

Fig. 2 Indentation residual depths of CN_x films using the Hysitron tester.

Fig. 3 The rms. of CNx films within a $2\mu\text{m} \times 2\mu\text{m}$ scan size using the Hysitron tester.

Fig. 4 Wear depths of CNx films with $23\ \mu\text{N}$ load after 1 cycle using the PCM.

Fig. 5 Wear depths of CNx films with $63\ \mu\text{N}$ load after 1 cycle using the PCM.

Fig. 6 Wear depth versus wear cycle on the DLC film using the PCM.

Fig. 7 “Bump-type” textured wear mark on the DLC film.

Fig. 8 Wear mark on the DLC film after 20 wear cycles.

Fig. 9 Wear depths of nano-fatigue wear tests with $15\ \mu\text{N}$ load and 2000 wear cycles.

Fig.10 Frictional build-up on the p-type Si with a orientation of $\langle 111 \rangle$.

Fig.11 “Reference coordinate system” was placed on the bare Si $\langle 100 \rangle$ using a etching process.

Fig.12 Frictional build-up observed under the PCM.

Fig.13 The same frictional build-up was observed under the commercial AFM.

Fig.14 Nano-fatigue wear tests on Si $\langle 100 \rangle$ under various environment.

References

1. Miyamoto, T., Miyake, T., and Kaneko, R., 1993, “Wear resistance of C^+ -implanted silicon investigated by scanning probe microscopy”, *Wear*, Vol. 162-164, pt. B, pp.733-738
2. Jiang, Z., Bogy, D. B., and Jahanmir, S., 1995a, “Nano-wear”, *CML Technical Report, ASME J. of Tribology*, submitted.

3. Jiang, Z., Hsiao, R., and Bogy, D.B., 1995b, "Nano-fatigue wear and frictional material build-up caused by repeated nano-frictional sliding", *CML Technical Report*, No. 95-008.
4. Jiang, Z., Hsiao, R., and Bogy, D.B., 1995c, "Nano-fatigue wear", *CML Technical Report*, No. 95-023, *ASME J. of Tribology*, submitted.
5. Jiang, Z., Lu, C.-J., Bogy, D.B., Bhatia, C.S., and Miyamoto, T., 1995e, "Nanotribological characterization of hydrogenated carbon films by scanning probe microscopy", *Thin Solid Films*, Vol.258, pp. 75-81.
6. Miyamoto, T., Serikawa, T., Hirono, S., Jiang, Z., Bogy, D.B., and Kaneko, R., 1995, "Tribological characterizations of SiO₂ films investigated by scanning probe microscopy", *IEEE Transactions on Magnetics*, Vol.31, No.6, pp.3018-3020.
7. Khurshudov, A. and Kato, K.,1995, "Wear mechanism in reciprocal scratching of polycarbonate, studied by atomic force microscopy", *Wear*.

Acknowledgments

This research was supported by the Computer Mechanics Laboratory at the University of California at Berkeley. The authors are grateful to Dr. Patrick Cheung for his technical support with the sample etching process at the University of California at Berkeley.

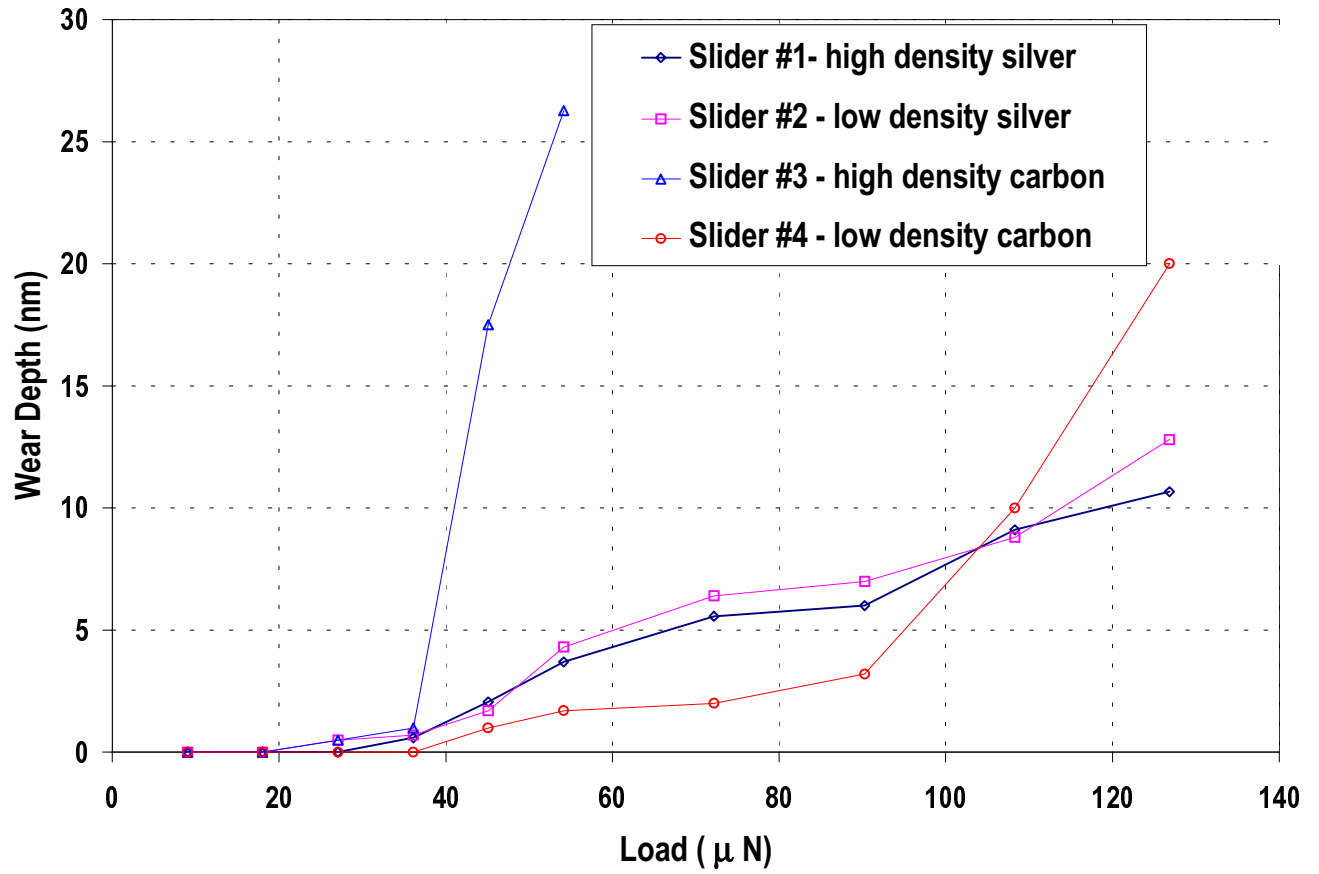


Fig. 1: Wear depth versus loading force on carbon and silver coated sliders.

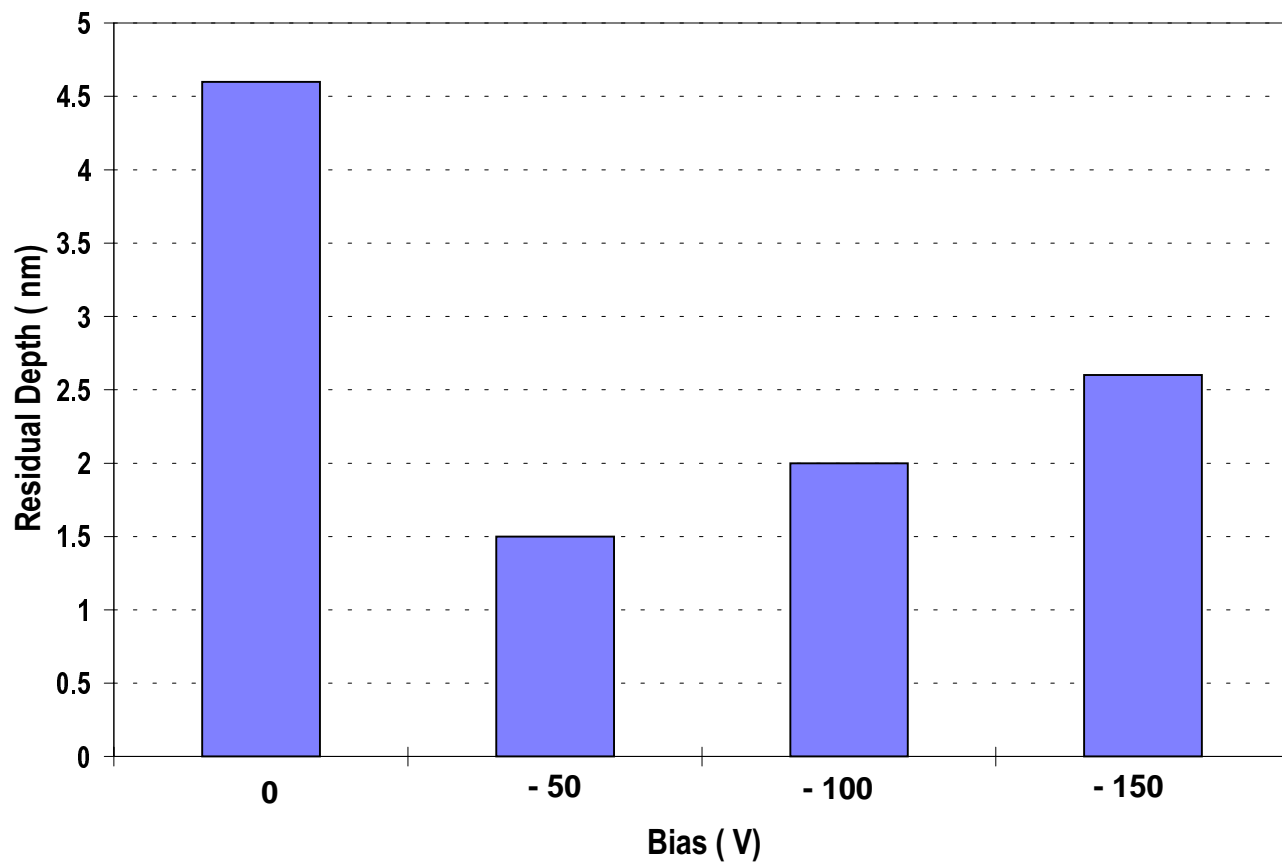


Fig. 2: Indentation residual depths of the CNx films using the Hysitron tester.

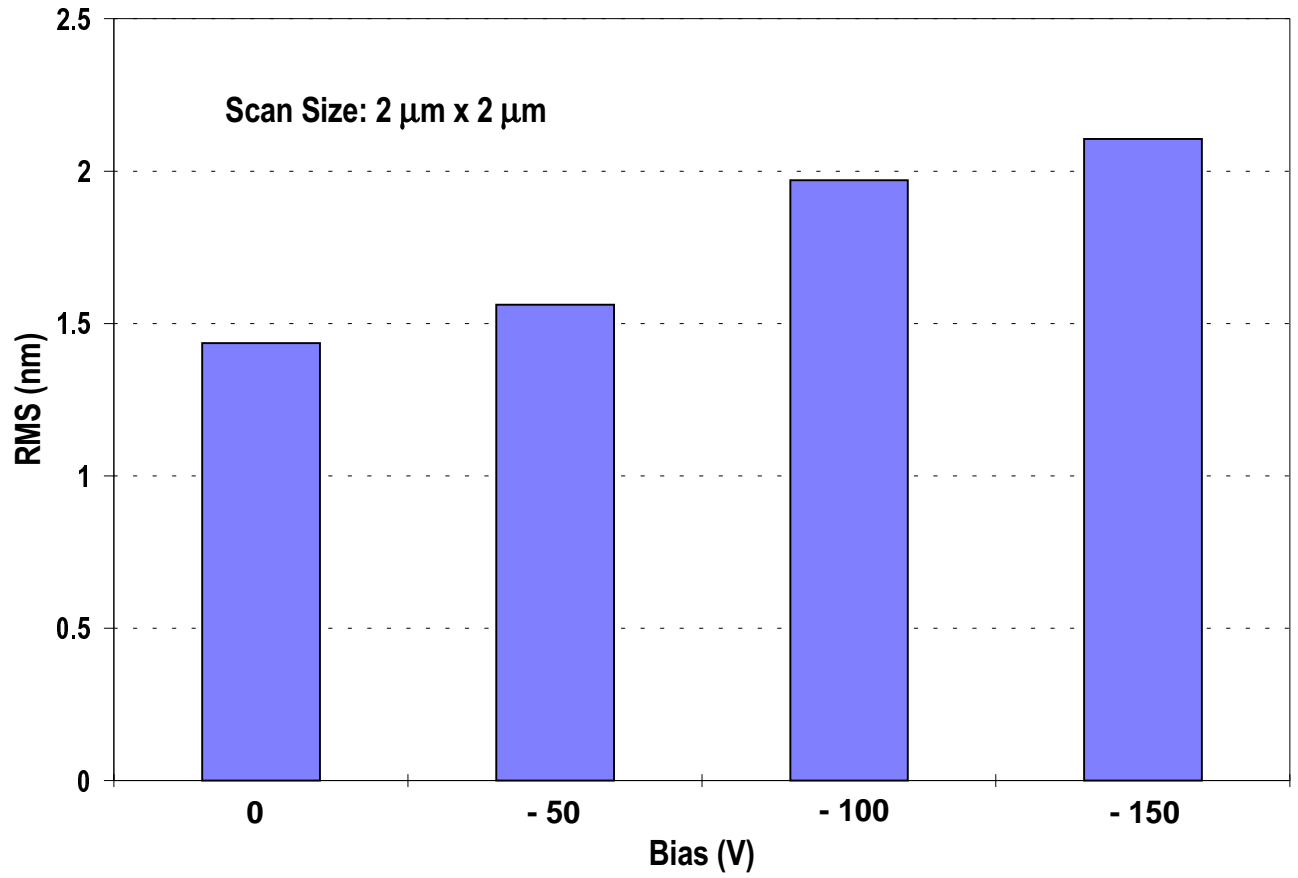


Fig. 3: Rms surface roughness of the CNx films with a 2 μm \times 2 μm scan size using the Hysitron tester.

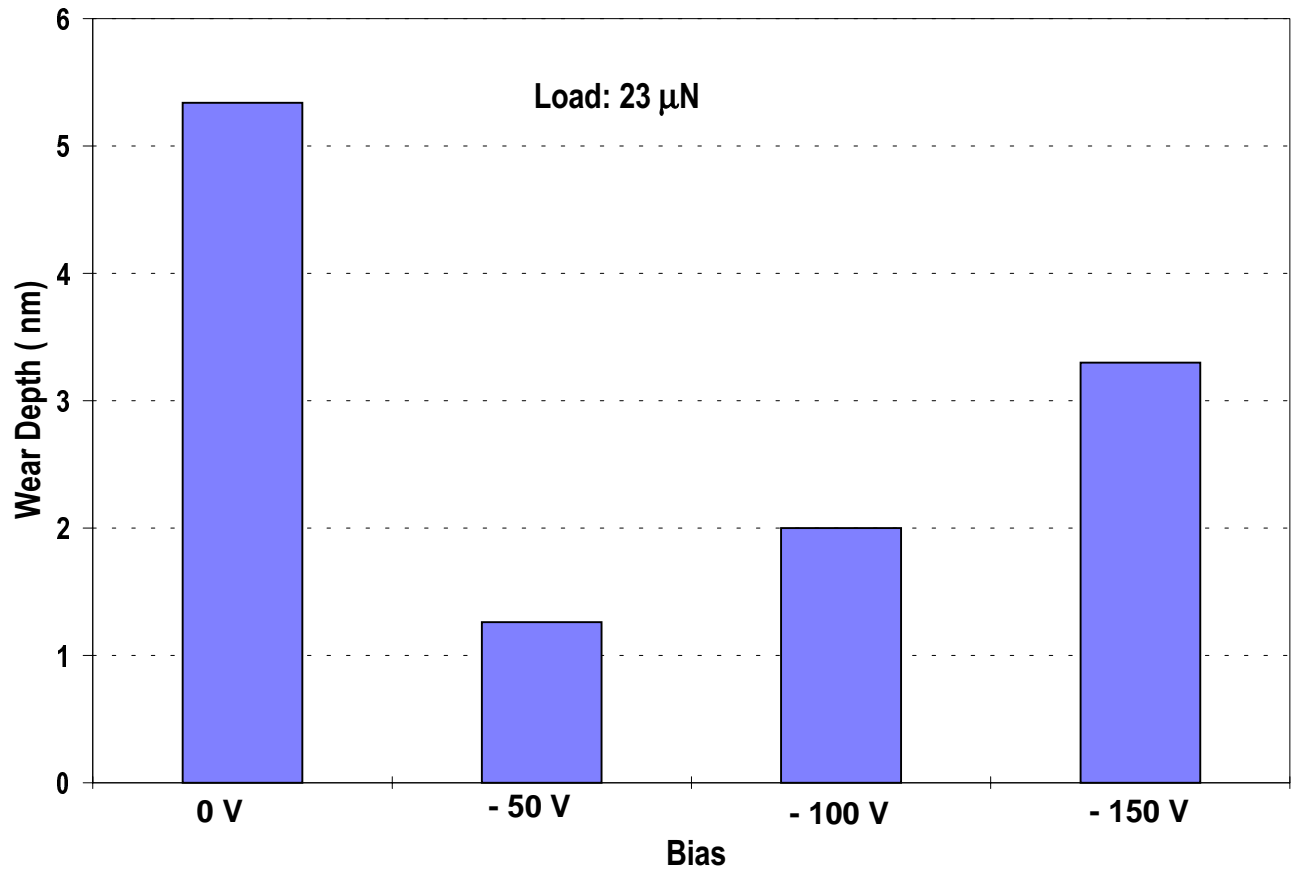


Fig. 4 : Wear depths of the CNx films with 23 μ N load after 1 cycle of nano-wear test using the PCM.

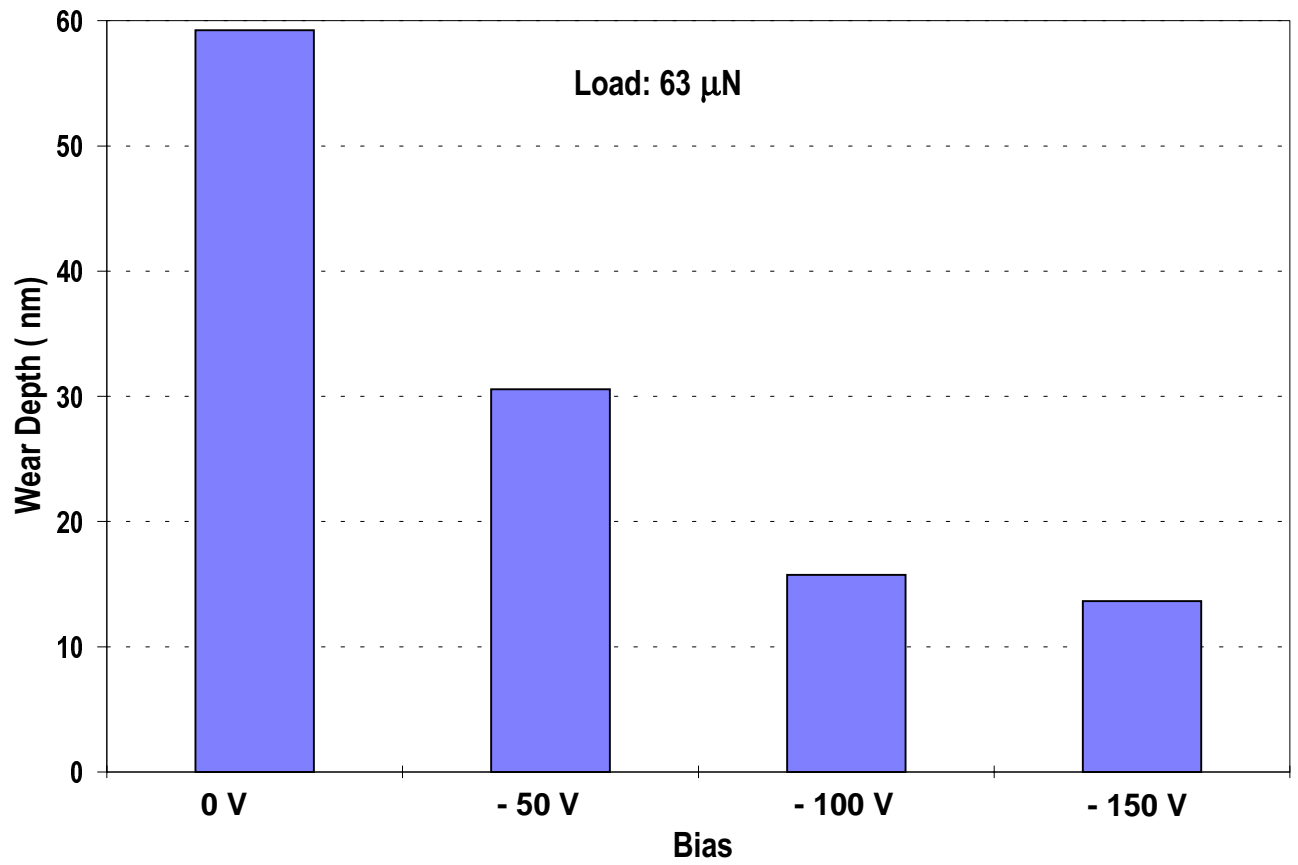


Fig. 5 : Wear depths of the CNx films with 63 μ N load after 1 cycle of nano-wear test using the PCM.

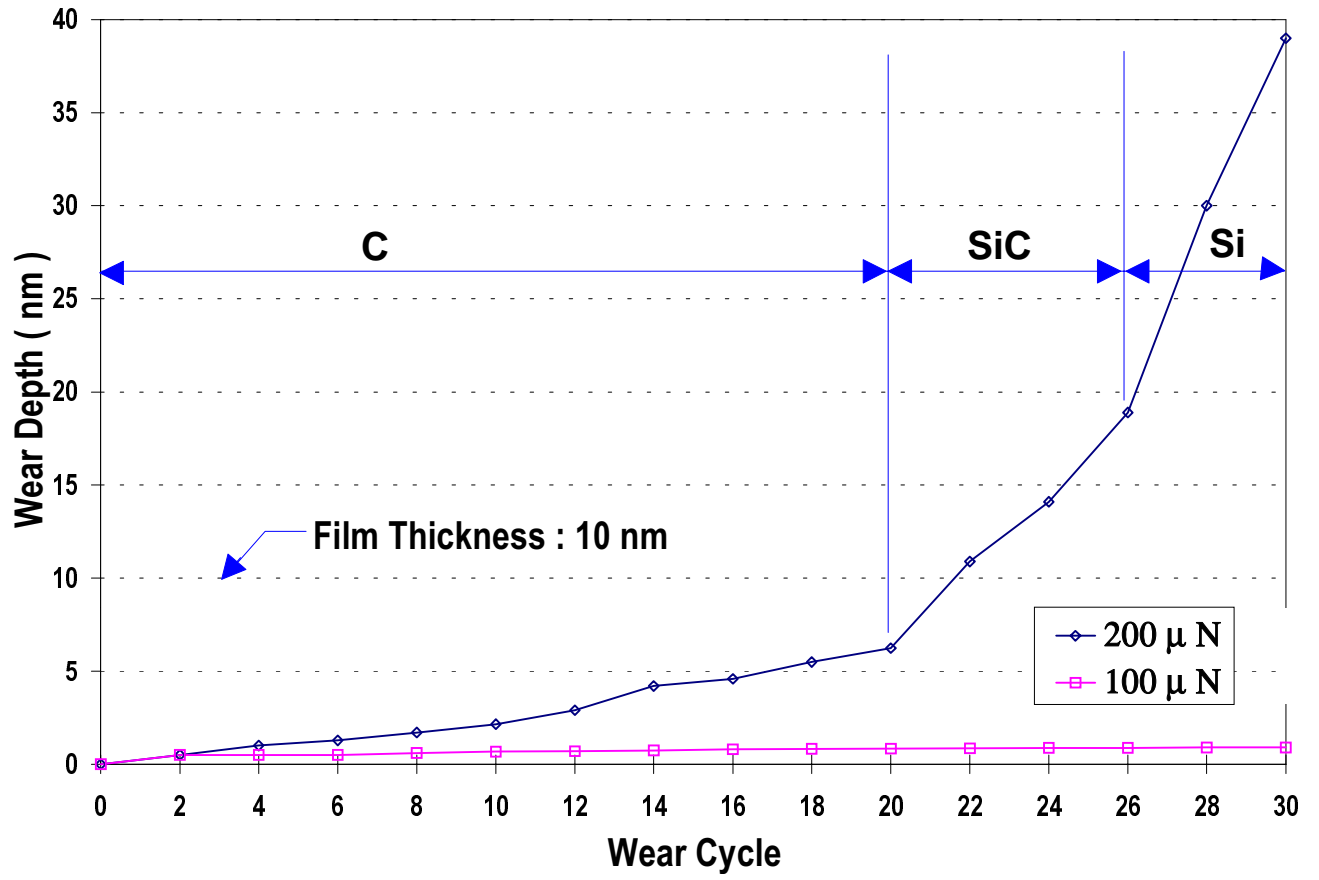


Fig. 6 : Wear depth versus wear cycle on the DLC film using the PCM.

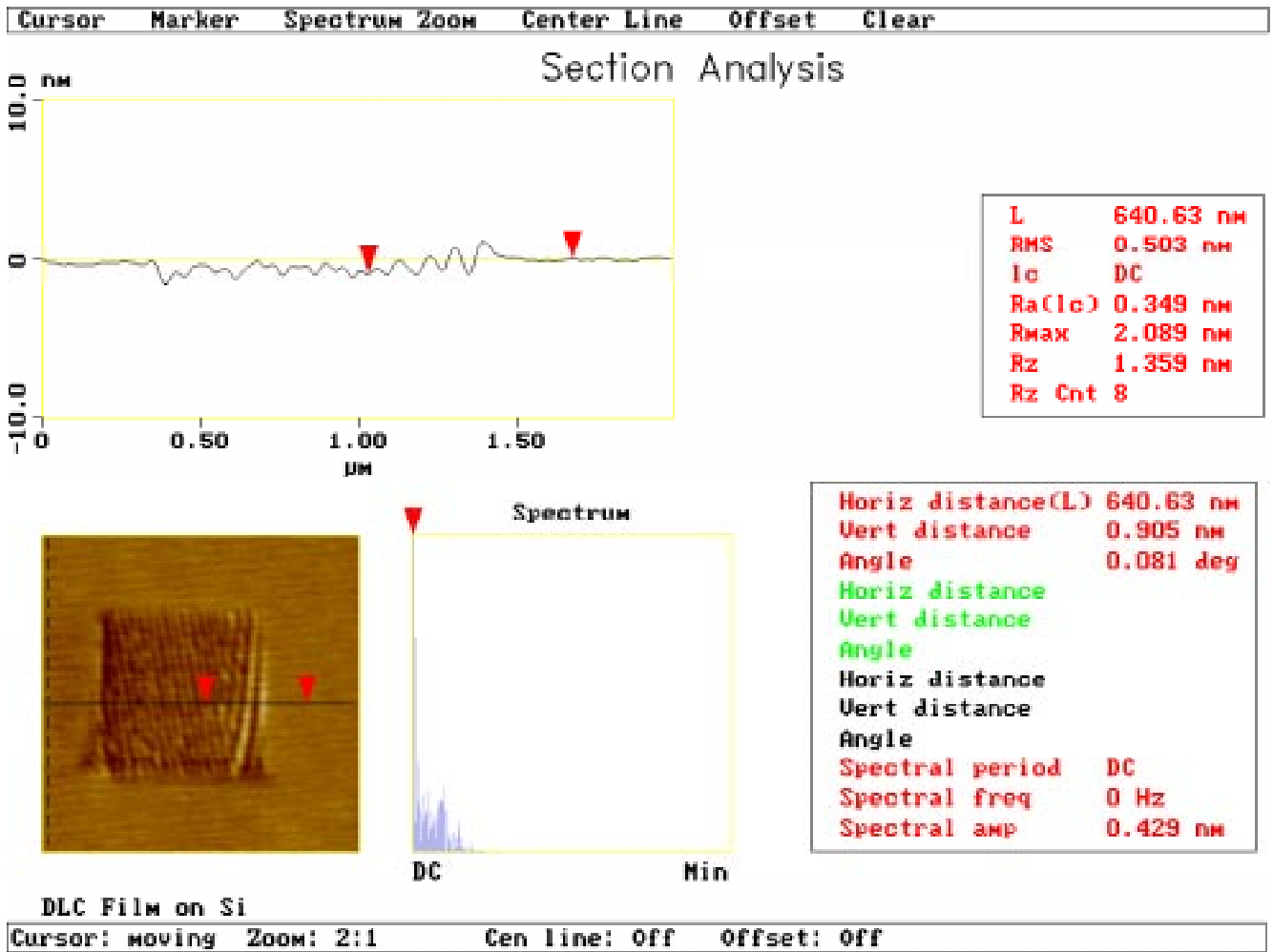


Fig. 7: Bump-type textured wear mark on the DLC film.

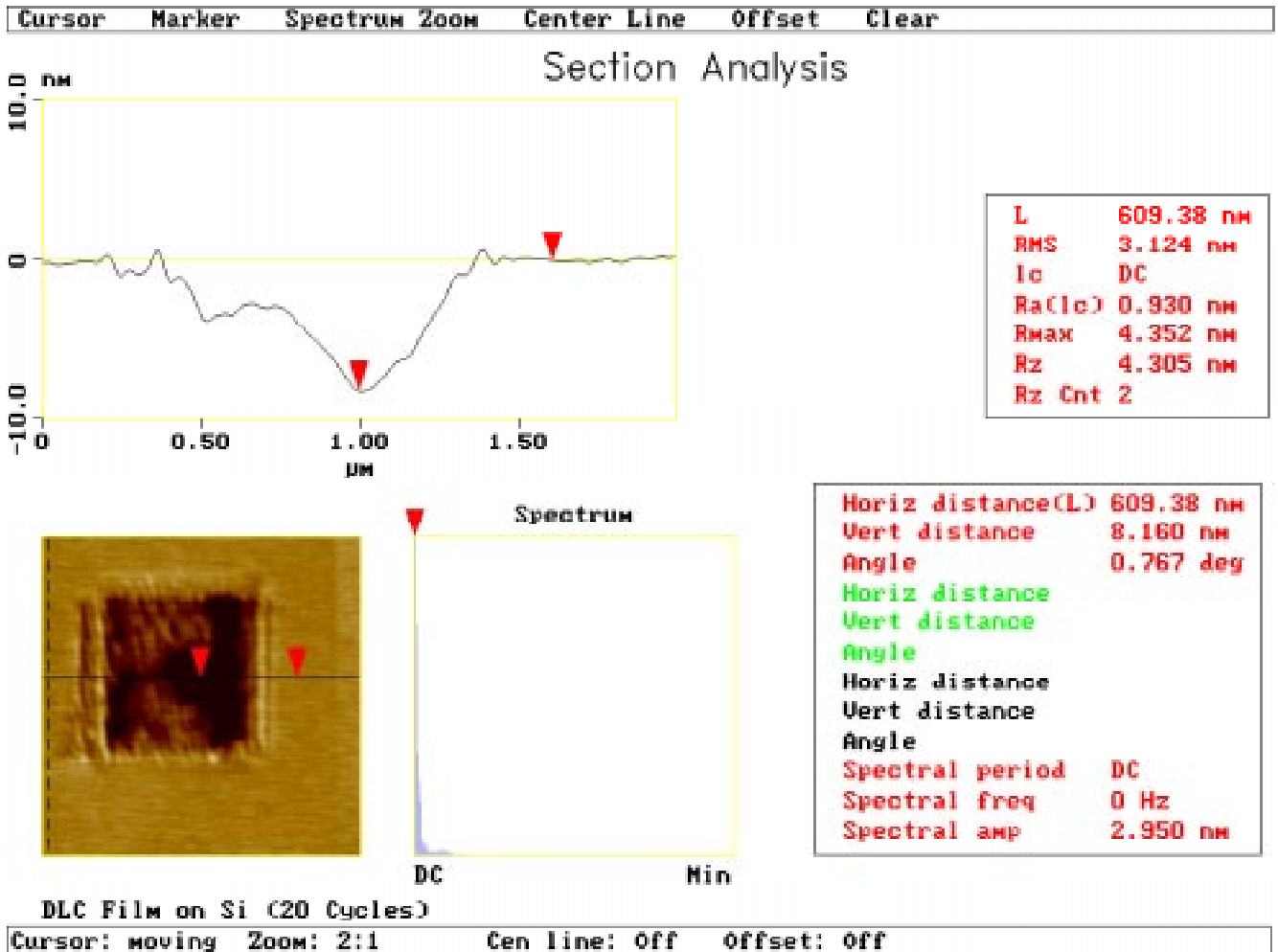


Fig. 8: Wear mark on the DLC film after 20 wear cycles.

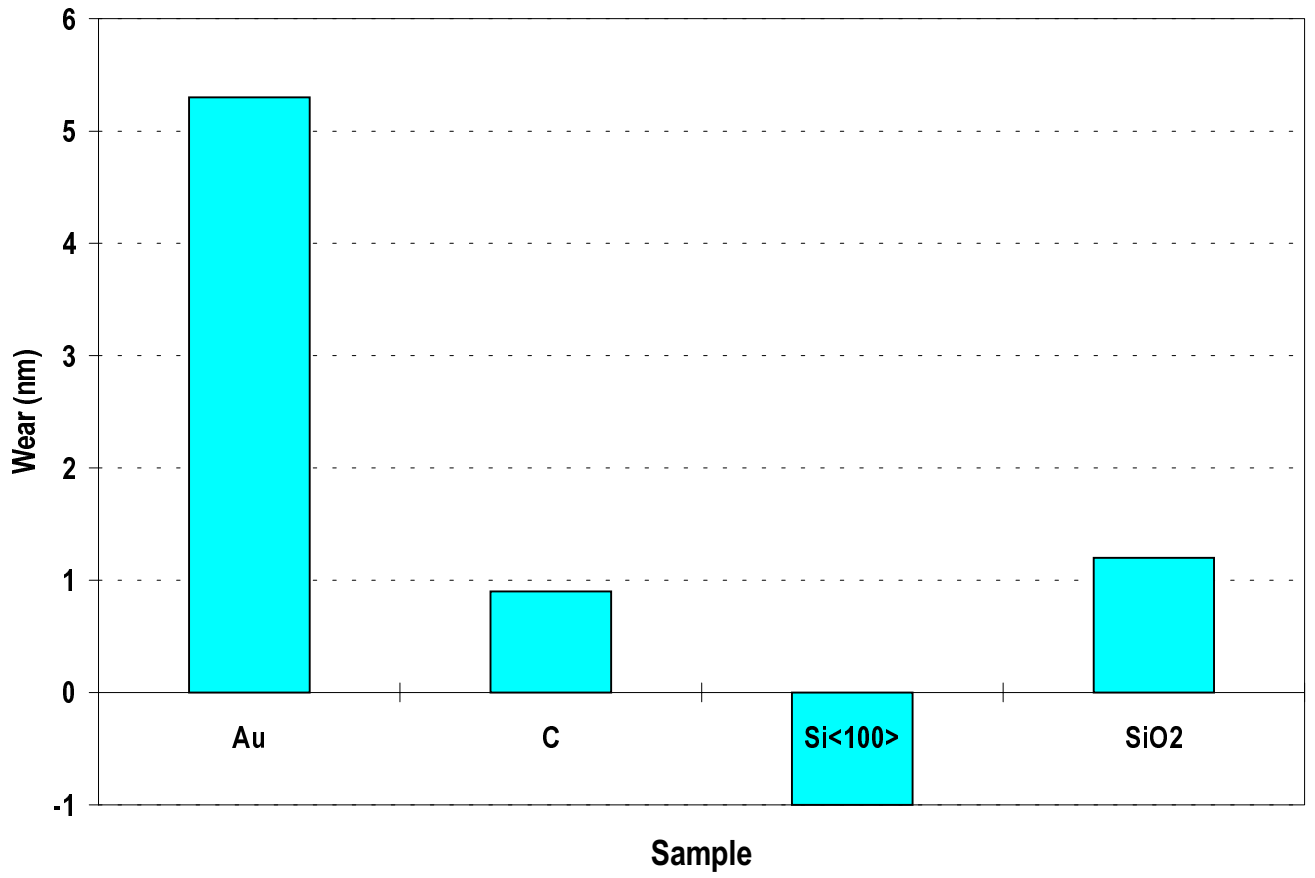


Fig. 9 : Wear depths of nano-fatigue wear tests with 15 μN load and 2000 wear cycles.

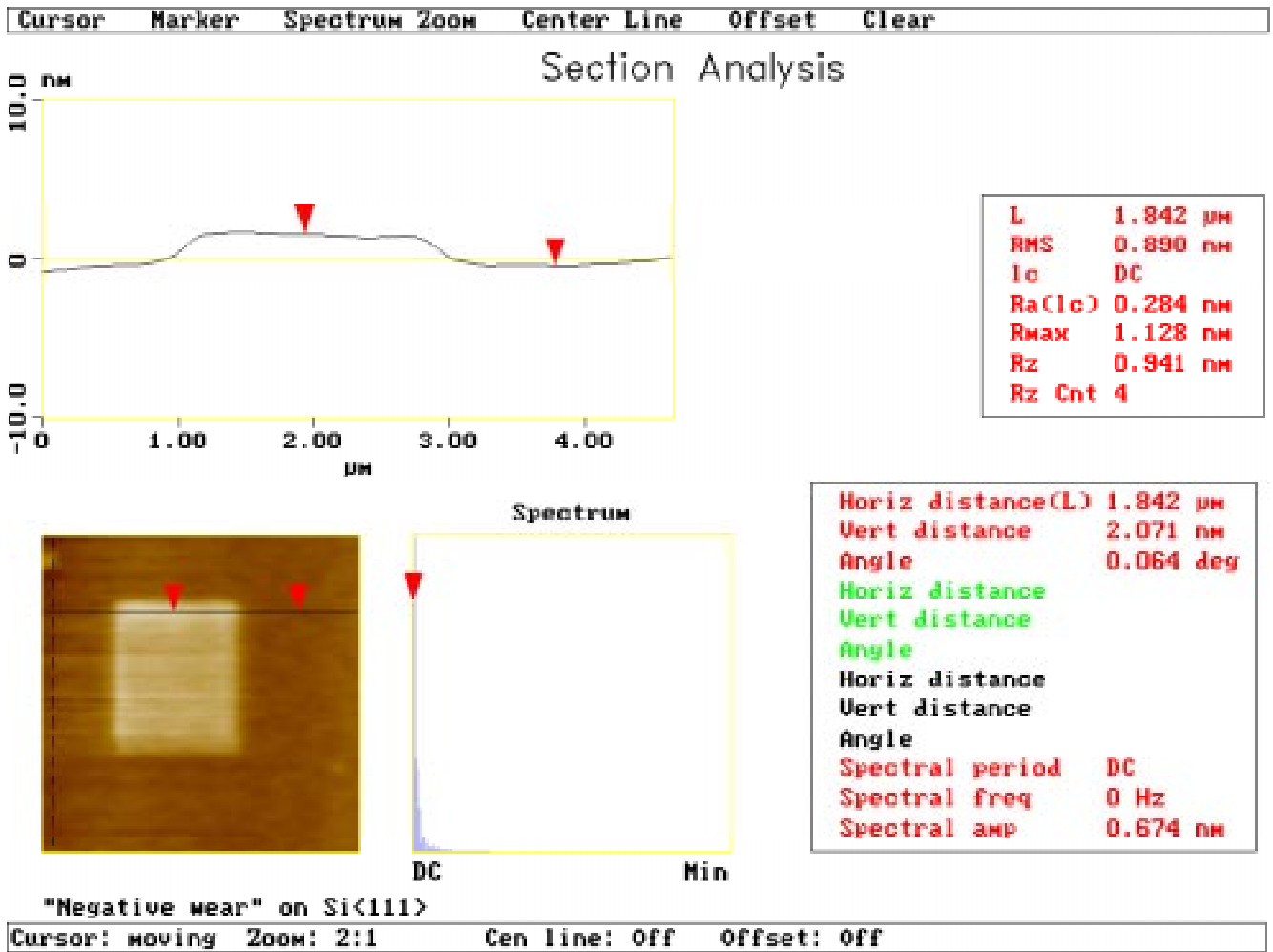


Fig. 10: Frictional patch on the p-type Si with a orientation of <111>.

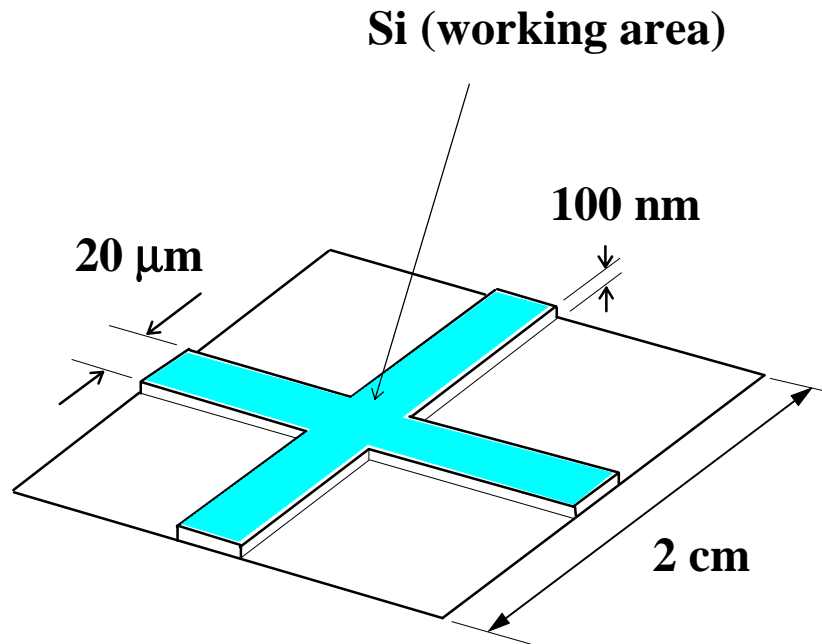


Fig. 11: "Reference coordinate system" was placed on the bare Si<100> using the etching process.

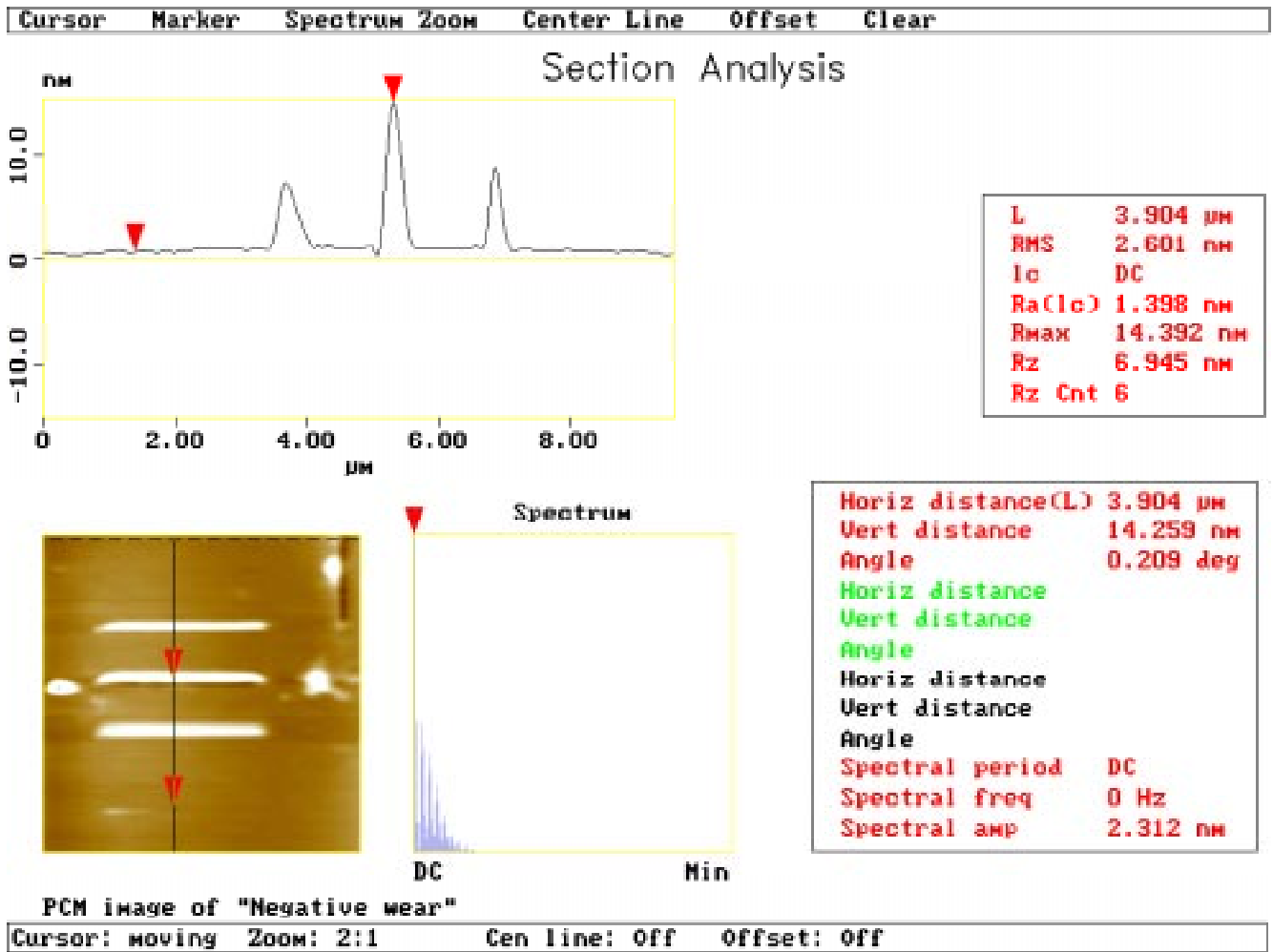
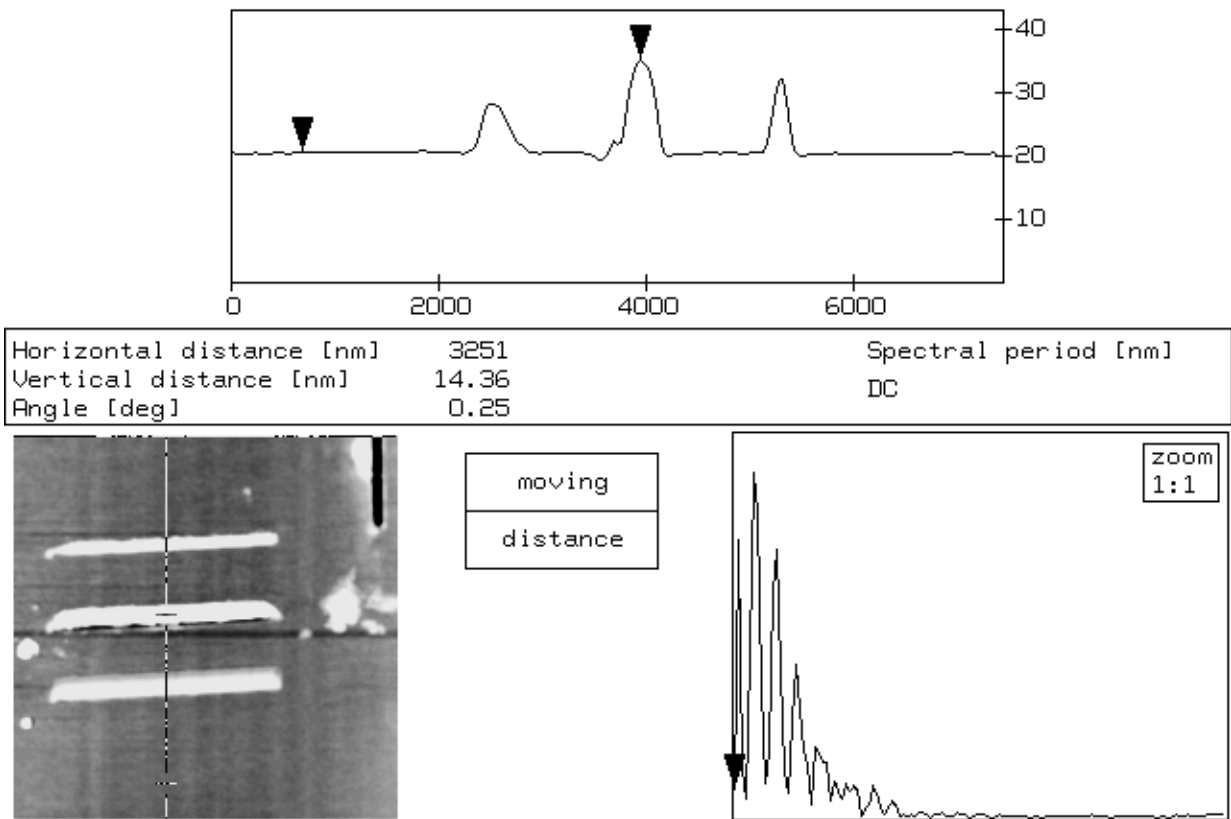


Fig. 12: Frictional build-up observed under the PCM.



Buffer 1(CORNER1A@), Rotated 0°, XY axes [nm], Z axis [nm]

Fig. 13: The same frictional build-up was observed under the commercial AFM.

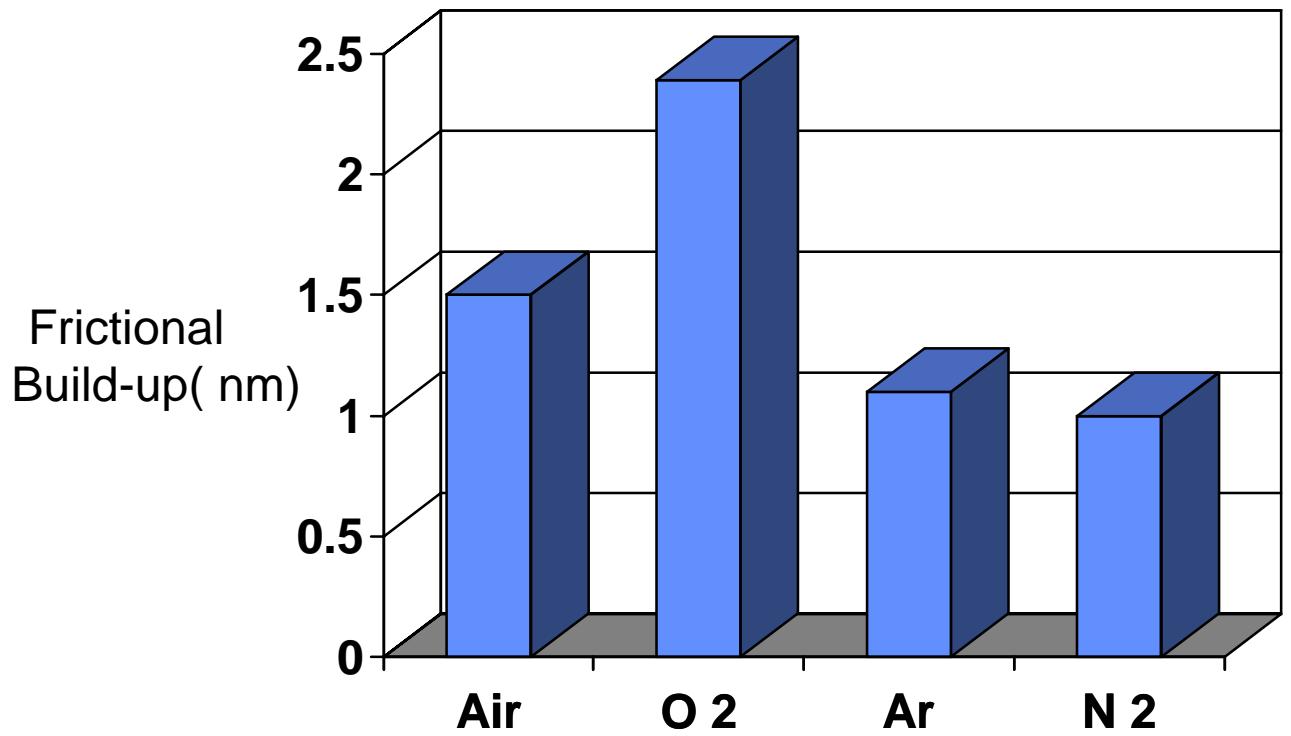


Fig. 14: Nano-fatigue wear tests on Si<100> under various environments.